View Article Online
View Journal

CrystEngComm

Accepted Manuscript

This article can be cited before page numbers have been issued, to do this please use: D. Tan, Z. X. Ng, S. Ying, R. Ganguly and F. Garcia, *CrystEngComm*, 2018, DOI: 10.1039/C8CE00395E.

Volume 18 | Number 1 | 7 January 2016 | Pages 1–184

CrystEngComm

www.rsc.org/crystengcomm

ROYAL SOCIETY OF CHEMISTRY

HIGHLIGHT
Tiddo J. Mooibroek, Antonio Frontera et al.
Towards design strategies for anion–π interactions in crystal engineering

175 YEARS

ROYAL SOCIETY OF CHEMISTRY

rsc.li/crystengcomm

View Article Online
DOI: 10.1039/C8CE00395E

Journal Name

COMMUNICATION

Cis-cyclodiphosph(V/V)azanes as Highly Stable and Robust Main Group Supramolecular Building Blocks

Received 00th January 20xx,
Accepted 00th January 20xx

DOI: 10.1039/x0xx00000x

www.rsc.org/

Davin Tan,[a] Zi Xuan Ng,[a] Ying Sim,[a] Rakesh Ganguly[a] and Felipe García [a,]*

Cyclophosphazanes have been extensively studied over the past decades due to their topological flexibility and unique chemical versatility. However, their use in supramolecular chemistry and crystal engeneering is still in its infancy. Here, we report the synthesis of *cis* Se-oxidized cyclodiphosph(V/V)azane 1 as a model cyclophosphazane compound, and its use as supramolecular building blocks. The displayed *cis*-conformation, along with its tendency to adopt an *exo*, *exo* configuration of the terminal *tert*-butylamino substituents, enables the formation of highly reproducible supramolecular synthons *via* $R^2_1(8)$ bifurcated hydrogen bonds. Such bifurcated hydrogen bonds formed by the cyclodiphosphazane scaffold contain larger bite angles than their more well-known urea, thiourea and squaramide counterparts. We obtained five different solvate crystals, as well as three different cocrystals that all contain similar hydrogen bonding motifs. In addition, we envisioned that the Se atoms in the oxidized cyclodiphosph(V/V)azane can act as halogen bonding acceptors, and we were able to successfully obtain a cocrystal with 1,4-dibromo-tetrafluorobenzene, *via* the formation of P=Se···Br halogen bonds. Such interaction had only been reported once before and warrants further exploration. Our results demonstrate the versatility and robustness of the cyclodiphosph(V/V)azane scaffold and highlights their potential as prospective building block for creating reproducible supramolecular synthons for main group crystal engineering purposes.

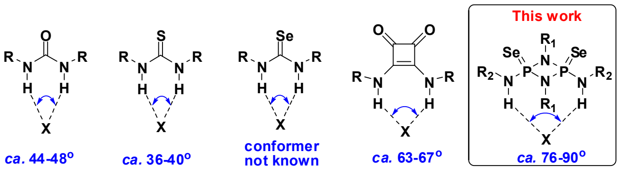

Figure 1. Various bifurcated hydrogen bond angles of ureas, thioureas, squaramides and herein presented work.

Introduction

Cyclophosphazanes, $[XP(\mu\text{-NR})]_n$ where X = halogen, amino or alkoxy and R = alkyl or aryl groups, are a rich family of cyclic arrangements comprising alternating phosphorus and nitrogen atoms.[1] Their size (*n*) – four-, six- or eight-membered ring – is dictated by the size of the amino substituent. Sterically bulkier moieties (*e.g.*, *tert*-butyl or *iso*-propyl) favours the formation of four-membered rings, while smaller substituents (*e.g.*, CH_3 or H) give rise to larger eight-membered rings.[2-5] Cyclodiphosphazanes, also known as diazadisphosphetidines,[6] are four-membered P_2N_2 cyclic species, have been successfully implemented in applications including coordination chemistry,[7-10] host-guest chemistry,[11] anionic recognition,[12] macrocycle formation and rearrangements,[13-16] as well as catalysts for organic transformation reactions.[17,18] Despite their relatively straightforward syntheses, cyclodiphosph(III/III)azanes are prone to degradation by hydrolysis and oxidation, which impedes their broader use in areas requiring ambient conditions.[1,6] One strategy to circumvent such sensitivity to oxygen and moisture is to oxidize the phosphorus(III) centres to phosphorus(V) using chalcogen elements, for example S or Se. Our group recently reported systematic air- and moisture-stability studies of a series of functionalized cyclodiphosph(V/V)azane compounds,[19,20] in which both computational and experimental data indicate increased kinetic stability of the P_2N_2 ring – *i.e.* higher activation barrier, towards nucleophilic attack from water after oxidation (stability: unoxidised < O < S/Se).[19]

Within the cyclodiphosph(V/V)azane species, the *cis*-oxidized frameworks are of particular interest as they can adopt an *exo*, *exo* (Z, Z) conformation, where the two terminal NH moieties are oriented in a converging manner. Recently, Goldfuss *et al.* demonstrated that functionalized *cis*-oxidised cyclodiphosphazanes can be used for halide and acetate recognition[21] *via* hydrogen-bonding with the two NH groups. Such a motif is reminiscent of Etter's ureas[22] and thioureas,[23] whose molecular conformations are primed to form predictable intermolecular bifurcated hydrogen bonds in a $R^2_1(6)$ manner, as described by several groups.[24-26] However, the use of cyclodiphophazane scaffolds as similar supramolecular building blocks has yet to be widely established. Moreover, comparison

---

[a] *School of Physical and Mathematical Sciences, Division of Chemistry and Biological Chemistry, Nanyang Technological University, 21 Nanyang Link 637371, Singapore (Singapore)*

View Article Online
DOI: 10.1039/C8CE00395E

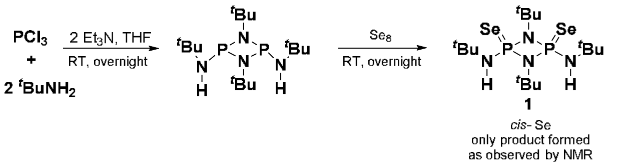

Figure 2. Selective formation of cyclophosph(V)azane **1** *via* a two-step synthesis. ^{31}P{^{1}H}-NMR only showed formation of the cis-oxidised product.

of the bifurcated hydrogen-bond bite angles, revealed that *cis*-oxidised cyclodiphosph(V)azane frameworks have larger bite angles than their urea, thiourea and squaramide counterparts (Figure 1),[27,28] which can be attributed to the formation of a larger sized $R^2_1(8)$ synthon. In this aspect, these *cis*-Se oxidised cyclodiphosph(V/V)azanes are considered desirable, to expand the number of examples of bifurcated hydrogen-bonding motifs with larger bite angles.

With this in mind, we set out to demonstrate the proof-of-concept that these frameworks can form robust and reliable hydrogen-bond synthons in the assembly of main group supramolecular arrangements.[29-31] For this purpose we implemented *cis*-Se oxidised tetrakis-*tert*-butyl-amino cyclodiphosph(V/V)azane **1** as a model molecule (Figure 2) to cocrystallise with various solid and liquid compounds.

Results and discussion

Solvate crystals of 1

Compound **1** was synthesised in bulk (8-10 g scale) *via* a two-step process, by first reacting distilled PCl_3, Et_3N and $^{t}BuNH_2$ in a 1:2:2 stoichiometric ratio in dry THF to afford the unoxidised symmetrically substituted cyclodiphosph(III/III)azane intermediate (Figure 2). The phosphorus(III) intermediate was not isolated and subsequently used for the next step. After removal of the triethylammonium chloride by-product, elemental Se was added as an oxidant. Overnight stirring at room temperature yielded the desired cyclophosph(V/V)azane compound. *In situ* ^{31}P{^{1}H} NMR spectroscopic studies revealed the exclusive formation of the *cis*-oxidised isomer (see SI), which has been shown to be highly stable when exposed to air and water over several weeks (see SI).[16-18,32]

Table 1. Screening of various solvents and solvent combinations for **1**.

S/N	Solvent	Crystals	S/N	Solvent	Crystals
1	acetone	yes, solvate	10	toluene	no, film
2	DMSO	yes, solvate	11	hexane	no, film
3	MeOH	yes, solvate	12	EA	no, film
4	^{i}PrOH	no, film	13	CH_3CN	yes, solvate
5	DMF	yes, solvate	14	1+2+8	solvate of 2
6	$CHCl_3$	no, film	15	3+7	solvate of 3
7	CH_2Cl_2	no, film	16	7+10	no, film
8	ether	insoluble	17	1+4	solvate of 1
9	THF	no, film	18	6+8	no, film

The structure of **1** was previously reported to adopt a *exo*, *endo* (*Z*, *E*) conformation (CSD code XOTGAO)[33] whereby one of the terminal *tert*-butyl groups is pointed outwards and one directed inwards. In our case, recrystallisation of the as-synthesized **1** in acetone readily formed crystals of the acetone solvate. Single-crystal X-ray diffraction (SCXRD) analysis revealed that the **1**:acetone adopted an *exo*, *exo* (*Z*, *Z*) conformation instead. In this conformation, both terminal *tert*-butyl groups point away from one another, and the NH groups are oriented inwards, forming $R^2_1(8)$ bifurcated hydrogen bonds with the solvate molecule. Subsequently, 18 different solvents and solvent combinations, with varying polarities and functional groups, were screened (Table 1) in order to determine which solvate crystals of **1** would form, and whether their packing motifs would be similar. The DMSO solvate of **1** (Table 1, entry 2) readily crystallises within 14 hrs, with excellent quality crystals of the solvate being obtained, despite growing crystals from a dilute solution. In fact, the **1**:DMSO cocrystal preferentially forms when using a combination of solvents (entry 14). Solvates of MeOH, DMF and CH_3CN (entry 3, 5, 13) were also obtained from their respective solutions. However, less polar solvents, for example $CHCl_3$ and toluene, formed only crusty films and, despite several attempts, did not afford any crystals suitable for diffraction studies.

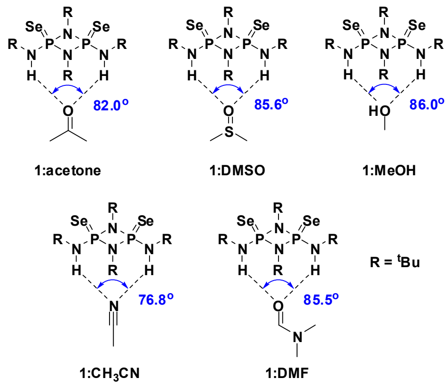

Figure 3. Cocrystallisation of **1** with different solvents.

As expected, the obtained solvates of **1** consisted of the same intermolecular $R^2_1(8)$ bifurcated hydrogen-bonding motif, as these solvent molecules contained polar functional groups that can act as hydrogen bond acceptors (see Figure 3), forming either N-H···N or N-H···O type hydrogen bonds, with relatively large bifurcated bite angles ranging from 76.8° (CH_3CN solvate) to 86.0° (MeOH solvate). For the MeOH solvate of **1**, the MeOH molecules can also act as hydrogen bond donors, whereby long range O-H···Se type hydrogen bonds (O···Se distance of 3.351 Å) between MeOH and neighbouring molecules of **1** was also observed. Fourier-transform infrared (FTIR) spectroscopic analysis was performed on the solvate crystals and

View Article Online
DOI: 10.1039/C8CE00395E

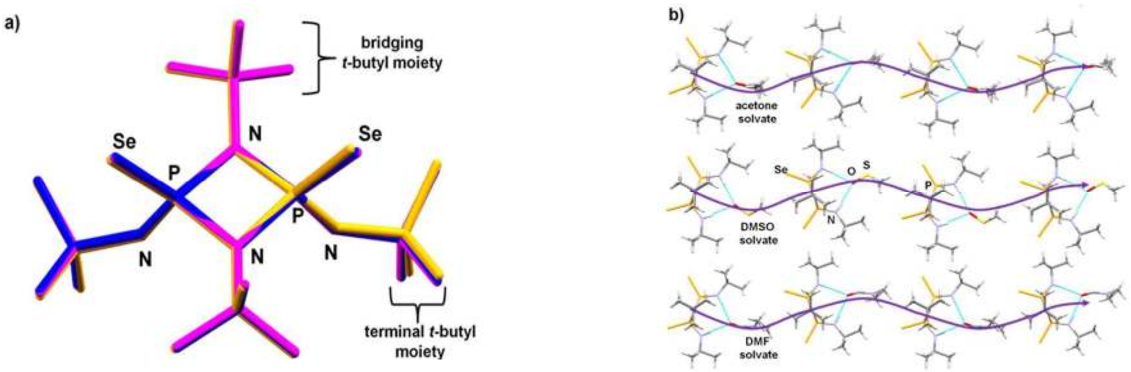

Figure 4. a) Overlay of the molecules of **1** as obtained from the SCXRD of the acetone (blue), DMSO (yellow) and DMF (magenta) solvate crystals. b) Hydrogen-bonded pairs of **1** with acetone, DMSO and DMF molecules. The similarly in the packing of the molecules, forming wavey chains (purple lines) clearly illustrates isostructurality between the three solvate crystals. Hydrogen atoms are omitted for clarity.

compared with those that formed films (see SI) which might suggest the presence of the bifurcated hydrogen bond formation in the solvate crystals but absent in the films. Further analysis of these five solvate crystals of **1** revealed interesting properties in their molecular arrangements. The *tert*-butyl groups on the bridging N of the P_2N_2 ring (endocyclic) and terminal ends (exocyclic) were observed to adopt an eclipsed conformation rather than a staggered one in most of the occasions (see SI Figure S11). This is unusual as one might reasonably assume that the eclipsed *tert*-butyl groups would be sterically disfavoured. Such preferred eclipsed conformation could be explained by crystal packing forces[34] that affects the overall configuration of the molecule. In addition, isostructurality was observed amongst the acetone, DMSO and DMF solvates (*i.e.*, identical space group (*P*nma) and packing motif, and almost identical unit cell parameters. See SI). Overlay of the molecular conformation of **1** derived from the three solvate crystals displayed almost perfect superposition of all the atoms (Figure 4a) which denotes the isostructurality of the three solvates. This is not surprising since the three solvent molecules are very similar in shape, size, functional group and molecular volumes; thus, adhering to Kitaigorodskii's principle of close packing.[35] In addition, from the figure, it is clear that the *tert*-butyl groups of the bridging and terminal ends are eclipsed with one another. The three solvates of **1** formed hydrogen-bonded pairs, which in turn assembles to form wavey chains (Figure 4b); however, it is important to note that the associated pairs in the chains are not linked together.

Bifurcated hydrogen-bonded cocrystals

In addition to solvate cocrystals, we investigated whether cocrystallisation with other liquid and solid coformers would result in similar bifurcated hydrogen bonding motif. For this purpose, 1,1,3,3-tetramethyl-guanidine (TMG) was chosen as the first cocrystal former candidate. TMG, a liquid at ambient temperature, is known to act as a strong organic base.[36] Therefore, TMG is expected to deprotonate the NH moieties present in **1** to afford the corresponding salt ion pair.

Crystals suitable for diffraction studies were readily obtained from a variety of solvents (see SI). Our studies revealed the cocrystallisation of TMG and **1** in a 1:1 ratio displaying analogous $R^2_1(8)$ bifurcated hydrogen-bonding interactions with the five solvate molecules (*vide supra*). Surprisingly, the TMG was not protonated – a cocrystal was obtained and not a salt ion pair (see SI) – as was originally anticipated. Analysis of the molecular structure revealed that the both terminal P-N bond lengths are 1.628 and 1.633 Å respectively, which indicates P-N single bonds, and thus neither N-H moieties are deprotonated. This is unusual, as cocrystallisation with TMG usually forms ionic salts, due to the inherent strong basicity of TMG which tends to deprotonate acidic moieties.[36] To the best of our knowledge, the obtained cocrystal TMG:**1** is the first non-metal containing crystalline compound in which TMG is neutral and not protonated.[37] Furthermore, the bite angle of the bifurcated hydrogen bond of the cocrystal is also relatively large, up to 86.8°, and is larger than those of the solvates (Figure 3).

The TMG:**1** cocrystal (*P*bca) also adopts similar molecular packing motifs with the acetone, DMSO and DMF solvates (*P*nma). The only noticeable difference was the presence of alternating TMG:**1** pairs rotated about *ca.* 90° along the chain (see SI); and, thus, the TMG:**1** cocrystal is not isostructural with the other three solvates (*i.e.* acetone, DMSO and DMF). Attempts to obtain the TMG:**1** isostructural polymorph, using different solvents or solvent combinations, were unsuccessful - yielding only the characterised *P*bca polymorph. Interestingly, recrystallisation using DMSO or DMSO solvent combinations consistently yielded the DMSO solvate crystals of **1**.

Encouraged by the positive results obtained with TMG, we explored cocrystallisation of **1** and *N*,*N*'-dimethylurea (DMU) – which has a very similar shape and size to TMG. However, since DMU can act simultaneously as both hydrogen-bond acceptor and donor, we anticipated the formation of hydrogen-bonded catemeric chains upon cocrystallisation of DMU with compound **1**. We envisioned that such cocrystal catemers would be very similar to those of the homomeric urea chains, previously reported by Etter *et al.*[22] Diffraction quality crystals were successfully obtained by slow evaporation of solution mixtures using different solvents, which displayed a 1:1 stoi-

View Article Online
DOI: 10.1039/C8CE00395E

chiometric ratio of DMU and **1**. Similar to the cocrystallisation experiments involving TMG *vide supra*, when DMSO was used as part of the solvent mixture, the DMSO solvate of **1** was preferentially formed from the solution mixture; further demonstrating the unusual strong affinity of **1** for this solvent molecule.[38]

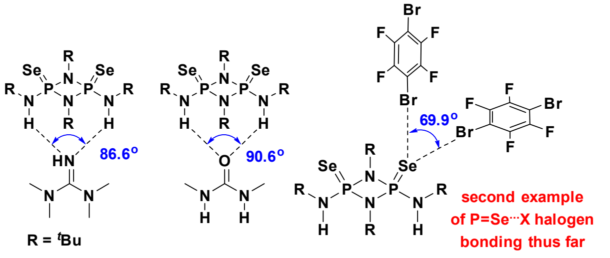

second example of P=Se···X halogen bonding thus far

Figure 5. Cocrystallisation of **1** with cocrystal formers forming bifurcated hydrogen and halogen bonds.

Two different polymorphs of DMU:**1** were obtained from MeOH and $CHCl_3$ solutions. Cocrystals were obtained by slow evaporation in MeOH and $CHCl_3$ afforded polymorph **I** and polymorph **II** respectively - with the bridging and terminal *tert*-butyl groups both adopting eclipsed conformations. Closer inspection of the structural parameters of these polymorphs revealed linear hydrogen-bonded chains comprising $R^2_1(8)$ bifurcated $(N\text{-}H)_2\cdots O$ (type X) and $R^2_2(10)$ non-bifurcated NH···Se (type Y_1) interactions in both cases (Figure 6). In general, the planar DMU molecules (orange) are aligned perpendicularly to the cyclodiphosphazane (blue) N-P-Se plane, forming large bite angles of up to 90.6°. In polymorph **I**, compound **1** and the DMU molecule form a repeating unit; with subsequent units being perpendicular (rotated approximately 90°) to one another as the chain propagates. Each repeating unit is linked by two long-range weak urea NH···Se interactions – with N-Se distance of 3.462-3.504 Å. Similarly, in polymorph **II**, the repeating units twist approximately 90° to one another as they grow along the chain. However, each repeating unit is comprised of two sets of DMU:**1** units and are connected by two different N-H···Se hydrogen bonds, specifically the aforementioned type-Y_1 and a bis-bifurcated $(N\text{-}H)_2\cdots Se$ (type Y_2) interactions (3.856-4.313 Å). Such a large repeating unit can be considered as an expanded hydrogen-bonded domain consisting of dimeric robust sub-assemblies[39] of two molecules. The difference in the two molecular packing assemblies can also be observed by FTIR spectroscopy (see SI).

Overall, the obtained solvates and cocrystals demonstrate that the bifurcated hydrogen-bonding motif in **1** is highly robust and consistently reproducible, providing a reliable supramolecular synthon, with cocrystals consistently packing in an analogous manner.

Halogen-bonded cocrystal

Apart from hydrogen-bonding interactions, the use of halogen bond for the construction of robust and reliable supramolecular assemblies has garnered much attention in the crystal engineering research community in recent years.[31, 40] Such supramolecular halogen bonds are typically formed when electron rich heteroatoms (O-, N-, S-, *etc.*) of the halogen-bond acceptor can donate their electron density into the σ-hole of halogen atoms. The strength of the halogen-bond can be enhanced by introducing electron withdrawing substituents, such as perfluorinated groups, making the halogen atom more electron deficient.

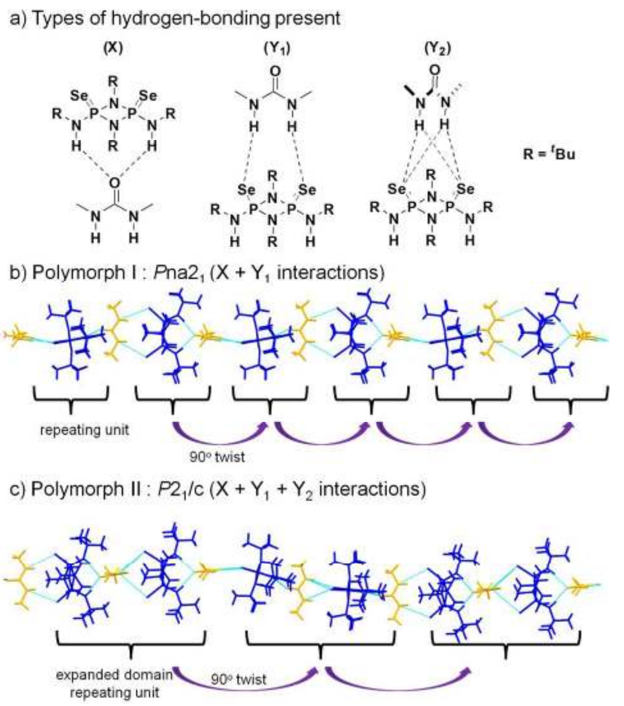

Figure 6. a) Three types of hydrogen-bonding interactions present for the 1:1 cocrystal of DMU (orange) and **1** (blue), namely bifurcated $(N\text{-}H)_2\cdots O$ (type X), N-H···Se (type Y_1) and bis-bifurcated $(N\text{-}H)_2\cdots Se$ (type Y_2). Polymorphs b) **I** and c) **II** of the cocrystal, forming hydrogen-bonded catemers. The repeating units along the chains are shown within brackets, with one associated pair in polymorph **I**, consisting of X- and Y_1-type hydrogen bonds, and two pairs in polymorph **II**, consisting of X-, Y_1- and Y_2-type hydrogen bonds. Polymorph **II** can be seen as an expanded domain of **I** consisting of dimeric sub-assemblies. Each subsequent unit in their respective polymorph is rotated about 90° as it propagates along their chains.

Whilst phosphine-oxide based halogen-bond acceptors have been previously reported,[41] halogen-bonding of the type P=Se···X (where X= Br, I) are still relatively unexplored. Seminal work from Pennington and Bayse has demonstrated the formation of halogen-bonding interactions between triphenylphosphine(V)selenide and organoiodides[42] – providing the first example of rationally designed P=Se···X halogen bonds. To further expand this class of halogen-bonded phosphine-selenide species, and provide insights on the ability of cyclodiphosph(V/V)azanes to function as halogen-bond acceptors, we attempted the cocrystallisation of our model compound **1** with 1,4-dibromo-tetrafluorobenzene (DBTFB). As both **1** and DBTFB can act as bidirectional dual halogen-bond acceptor and donor respectively, we hypothesized that their cocrystal would lead to the formation of linear one-dimensional (1D) halogen-bonded chains. Successful cocrystal

View Article Online
DOI: 10.1039/C8CE00395E

formation would also further serve to demonstrate the versatility and robustness of the cyclodiphosphazane scaffold as supramolecular building blocks.

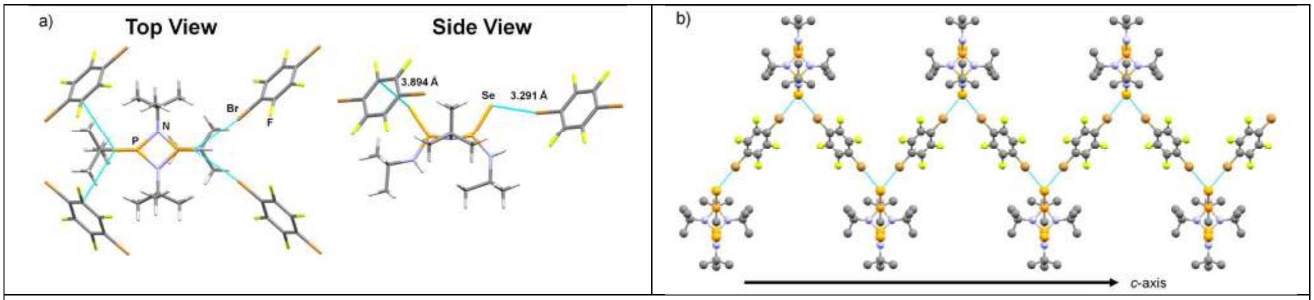

Figure 7. a) Top and side view of the capped-stick representation of the cocrystal between **1** and DBTFB. The endo Se forms bifurcated halogen-bonds (Se···Br distance 3.291 Å) while the exo Se forms Se···π interactions (Se···C distance 3.894 Å) with the electron deficient phenyl ring. b) Ball-and-stick representation of a fragment of the halogen-bonded corrugated chains formed between **1** and DBTFB.

The cocrystals of DBTFB with **1** in a 1:1 stoichiometric ratio was readily obtained in $CHCl_3$. SCXRD analysis of the molecular Conformation of **1**, revealed that **1** did not adopt the *exo*, *exo* (*Z*, *Z*) arrangement, but rather the *exo*, *endo* (*Z*, *E*) conformation (Figure 7) instead – identical to the XOTGAO structure *vide supra*.[33] This can be explained by the fact that in the absence of strong hydrogen bond acceptors such as the cocrystal formers and polar solvents *vide supra*, the cyclodiphosphazanes would adopt the *exo*, *endo* (*Z*, *E*) configuration, so as to possibly minimize steric repulsion of the *tert*-butyl groups between neighbouring molecules.

Here, in this cocrystal, the Se atom on the *endo*-side undergoes bifurcated halogen-bonding with two molecules of DBTFB (Se···Br distance of 3.291 Å and Br···Se···Br angle of 69.9°). On the other hand, the Se on the *exo*-side forms two Se···π interactions (Se···C distance 3.894 Å) with the electron deficient phenyl rings of two DBTFB molecules. Such unsymmetrically different interactions with the symmetrical molecule of **1** prevent the formation of linear one-dimensional halogen bonded chains. Instead, these bifurcated halogen-bonding motifs between the *endo*-side of **1** and DBTFB molecules, form zig-zag like chains that propagate along the crystallographic *c*-axis (Figure 6). Such bifurcated halogen bonding motif is reasonable, considering the large size of the Se atom, which can accommodate two halogen bonding sites, to form the observed corrugated chains.

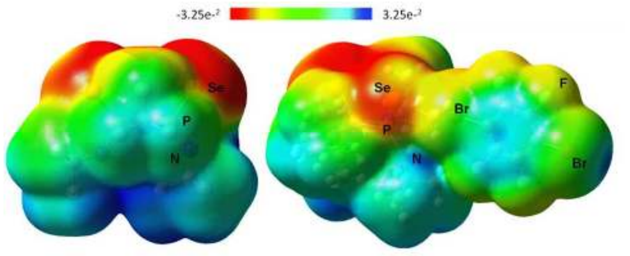

Figure 8. Electrostatic potential surface mapping, derived from the total self-consistent field density, of compound **1** (*left*) and of the **1**:DBTFB cocrystal (*right*), illustrating the halogen bond formed between the electron rich Se atom with the σ-hole of the Br atom. The coordinates were determined from SCXRD data. The color band denotes high electron density, as shown in reddish hues, contrasted with low electron density, as shown in blue hues.

Furthermore, electrostatic potential surface (ESP) derived from the mapping of **1** and the DBTFB:**1** cocrystal – based on atomic positions from SCXRD data – clearly indicate the high electron density present around the large Se atoms, as well as the lack of electron density around the phenyl rings and the σ-hole of the Br atom (Figure 8). From the ESP map, it is easy to deduce that the selenium atom is able to readily form the P=Se···Br halogen bonds by donating its electron density into the σ-hole of the electron poor Br atom of DBTFB (see Figure 8), as well as form the Se···π interactions.

Conclusions

In summary, we have shown the facile synthesis of a highly air- and moisture-stable *cis* Se- cyclophosph(V/V)azane, and demonstrated its use as a building block for the synthesis of a series of solvates and cocrystals using various “wet” bench-top solvents. These species undergo highly reproducible and robust $R^2_1(8)$ bifurcated hydrogen-bonding supramolecular synthons. We have successfully created associate pairs of alternating molecules of **1** with different coformers, including a series of solvates and two different cocrystals, namely TMG and DMU. In particular, cocrystallisation with DMU enabled the formation of two different polymorphic unidirectional hydrogen-bonded catemers.

Furthermore, halogen-bonding was also demonstrated when **1** was readily cocrystallized with DBTFB *via* formation of bifurcated P=Se···Br halogen bonds, which in turn self-assembles into 1D corrugated catemers. Such a phosphine-selenide based halogen-bonding motif is very rare[42] and warrants further investigation on the use of such motifs in supramolecular chemistry. We strongly believe that our presented results can be used as a platform to develop similar types of P=Se···Br halogen-bonded hybrid inorganic-organic systems, which within the main group arena, is only recently emerging. Our work underscores the suitability of *cis*-cyclophosph(V/V)azanes as new robust building blocks for creating hydrogen- and halogen-bonding supramolecular synthons. We hope that these results act as a stepping-stone for the development of new phosphazane building blocks towards more elaborate supramolecular arrangements and phosphazane-based hybrid inorganic-organic functional materials in the near future.

DOI: 10.1039/C8CE00395E

Conflicts of interest

The authors declare no conflict of interest.

Acknowledgements

F. García would like to thank NTU start-up grant (M4080552), and MOE Tier 1 grant (M4011441) for financial support. D. Tan would like to thank A*STAR AME IRG (A1783c0003) for PDRF. Z. X. Ng thanks the URECA program for studentship.

References

1 Balakrishna, M. S.; Eisler, D. J.; Chivers, T. *Chem. Soc. Rev.*, 2007, **36**, 650-664.
2 P. Chandrasekaran, J. T. Mague and M. S. A. Balakrishna, *Eur. J. Inorg. Chem.* 2011, 2264–2272.
3 R. Murugavel, G. Prabusankar, A. Sharma, R. B. Sunoj and R. J. Butcher, *Inorg. Chem.*, 2009, **48**, 2048-2059.
4 D. F. Moser, L. Grocholl, L. Stahl and R. J. Staples, *Dalton Trans.*, 2003, 1402–1410.
5 K. D. Gallicano, N. L. Paddock, S. J. Rettig, J. Trotter, *Can. J. Chem.*, 1982, **60**, 2415–2419.
6 M. S. Balakrishna, *Dalton Trans.*, 2016, **45**, 12252-12282.
7 M. Rastätter, R. B. Muterle, P. W. Roesky, and S. K.-H. Thiele, *Chem. Eur. J.*, 2009, **15**, 474-481.
8 T. Chivers, M. Krahn and G. Schatte, *Inorg. Chem.*, 2002, **41**, 4348-4354.
9 A. D. Bond, E. L. Doyle, F. García, R. A. Kowenicki, M. McPartlin, L. Riera and D. S. Wright, *Chem. Commun.*, 2003, 2990-2991.
10 A. D Bond, E. L. Doyle, F. García, R. A. Kowenicki, D. Moncrieff, M. McPartlin, L. Riera, A. D. Woods and D. S. Wright, *Chem. Eur. J.*, 2004, **10**, 2271-2276.
11 F. García, D. J. Linton, M. McPartlin, A. Rothenberger, A. E. H. Wheatley and D. S. Wright, *Dalton Trans.* **2002**, 481-483.
12 H. Klare, S. Hanft, J. M. Neudörfl, N. E. Schlörer, A. Griesbeck and B. Goldfuss, *Chem. Eur. J.*, 2014, **20**, 11847-11855.
13 F. García, R. A. Kowenicki, I. Kuzu, L. Riera, M. McPartlin and D. S. Wright, *Dalton Trans.*, 2004, 2904-2909.
14 F. Dodds, F. García, R. A. Kowenicki, M. McPartlin, A. Steiner and D. S. Wright, *Chem. Commun.*, 2005, 3733-3735.
15 A. Bashall, E. L. Doyle, F. García, G. T. Lawson, D. J. Linton, D. Moncrieff, M. McPartlin, A. D. Woods and D. S. Wright, *Chem. Eur. J.*, 2002, **8**, 5723-5731.
16 Y. X. Shi, K. Xu, J. K. Clegg, R. Ganguly, H. Hirao, T. Friščić and F. García, *Angew. Chem. Int. Ed.*, 2016, **55**, 12736-12740.
17 H. Klare, J. M. Neudörfl and B. Goldfuss, *Beilstein J. Org. Chem.*, 2014, **10**, 224–236.
18 M. E. Otang, G. R. Lief and L. Stahl, *J. Organomet. Chem.*, 2016, **820**, 98-110.
19 Y. X. Shi, R. Z. Liang, K. A. Martin, N. Weston, S. Gonzalez-Calera, R. Ganguly, Y. Li, Y. Lu, A. J. M. Ribeiro, M. J. Ramos, P. A. Fernandes and F. García, *Inorg. Chem.*, 2015, **54**, 6423-6432.
20 Y. Sim, D. Tan, R. Ganguly, Y. Li, and Felipe García, *Chem. Commun.* 2018, DOI: 10.1039/C8CC01043A.
21 F. F. Wolf, J. M. Neudörfl and B. Goldfuss, *New. J. Chem.*, 2018, http://dx.doi.org/10.1039/C7NJ04660J.
22 M. C. Etter and S. M. Reutzel, *J. Am. Chem. Soc.*, 1991, **113**, 2586-2598.
23 Y. Takemoto, *Org. Biomol. Chem.*, 2005, **3**, 4299-4306.
24 B. Som, J. R. Shue, M. D. Smith and L. S. Shimizu, *Acta Cryst.*, 2018, **C74**, 75–81.
25 C. Capacci-Daniel, S. Dehghan, V. M. Wurster, J. A. Basile, R. Hiremath, A. A. Sarjeant and J. A. Swift, *CrystEngComm*, 2008, **10**, 1875–1880.
26 R. Custelcean, *Chem. Commun.*, 2008, 295-307
27 Derived from reported structures in the Cambridge Structural Database (CSD), CCDC SEARCH date 10 March 2018, in CONQUEST version 1.21 on the 2018 database. Search parameters were limited to ureas, thioureas, selenoureas and squaramides that have free NH groups that can form bifurcated hydrogen-bonds.
28 Selenoureas only adopt a *trans*-conformation and thus hydrogen-bond bifurcation has yet to be reported in such species
29 C. B. Aakeröy, C. L. Spartz, S. Dembowski, S. Dwyre and J. Desper, IUCrJ, 2015, **2**, 498-510.
30 A. Mukherjee, S. Tothadi and G. R. Desiraju, *Acc. Chem. Res.*, 2014, **47**, 2514-2524.
31 G. Cavallo, P. Metrangolo, R. Milani, T. Pilati, A. Priimagi, G. Resnati, G. Terraneo, *Chem. Rev.*, 2016, **116**, 2478-2601.
32 A. J. Plajer, R. García-Rodríguez, C. G. M. Benson, P. D. Matthews, A. D. Bond, S. Singh, L. H. Gade and D. S. Wright, *Angew. Chem. Int. Ed.*, 2017, ***56***, 9087-9090.
33 T. Chivers, M. Krahn and G. Schatte, *Inorg. Chem.*, 2002, **41**, 4348-4354.
34 P. Dauber and A. T. Hagler, *Acc. Chem. Res.* 1980, **13**, 105-112.
35 A. I. Kitaigorodskii, *Acta Cryst.*, 1965, **18**, 585-590.
36 T. Ishikawa, *Superbases for Organic Synthesis: Guanidines, Amidines, Phosphazenes and Related Organocatalysts*, Wiley, Chippenham, 2009.
37 Derived from reported structures in the Cambridge Structural Database (CSD), CCDC SEARCH date 10 March 2018, in CONQUEST version 1.21 on the 2018 database. Search parameters include the TMG molecules (neutral and protonated), excluding those containing metal ions and/or metal complexes.
38 L. Spiteri, U. Baisch and L. Vella-Zarb, *CrystEngComm*, 2018, **20**, 1291-1303.
39 A. Tarai and J. B. Baruah, *New J. Chem.*, 2017, **41**, 10750-10760.
40 L. C Gilday, S. W. Robinson, T. A. Barendt, M. J. Langton, B. R. Mullaney and P. D. Beer, *Chem. Rev.*, 2015, **115**, 7118-7195.
41 S. Y. Oh, C. W. Nickels, F. García, W. Jones, T. Friščić, *CrystEngComm*, 2012, **14**, 6110-6114.
42 H. D. Arman, E. R. Rafferty, C. A. Bayse and W. T. Pennington, *Cryst. Growth Des.*, 2012, **12**, 4315−4323.